A Small Molecule Inhibitor, 1,2,4,5-Benzenetetraamine Tetrahydrochloride, Targeting the Y397 Site of Focal Adhesion Kinase Decreases Tumor Growth

Vita M. Golubovskaya,[†,‡] Carl Nyberg,[†,‡] Min Zheng,[†,‡] Frederick Kweh,[†,‡] Andrew Magis,[‡,§] David Ostrov,[‡,§] and William G. Cance*[,†,‡,||]

Department of Surgery, UF Shands Cancer Center, Department of Pathology and Laboratory Medicine, and Department of Biochemistry and Molecular Biology, University of Florida, Gainesville, Florida 32610-0245

Received April 25, 2008

Focal adhesion kinase (FAK) is a nonreceptor kinase that is overexpressed in many types of tumors. We developed a novel cancer-therapy approach, targeting the main autophosphorylation site of FAK, Y397, by computer modeling and screening of the National Cancer Institute (NCI) small molecule compounds database. More than 140 000 small molecule compounds were docked into the N-terminal domain of the FAK crystal structure in 100 different orientations that identified 35 compounds. One compound, **14** (1,2,4,5-benzenetetraamine tetrahydrochloride), significantly decreased viability in most of the cells to the levels equal to or higher than control FAK inhibitor **1a** (2-[5-chloro-2-[2-methoxy-4-(4-morpholinyl)phenylamino]pyrimidin-4-ylamino]-*N*-methylbenzamide, TAE226) from Novartis, Inc. Compound **14** specifically and directly blocked phosphorylation of Y397-FAK in a dose- and time-dependent manner. It increased cell detachment and inhibited cell adhesion in a dose-dependent manner. Furthermore, **14** effectively caused breast tumor regression in vivo. Thus, targeting the Y397 site of FAK with **14** inhibitor can be effectively used in cancer therapy.

Introduction

FAK[a] is a 125 kDa protein that localizes to focal adhesions[1] and is activated and tyrosine phosphorylated in response to integrin clustering.[2] Tyrosine 397 is an autophosphorylation site of FAK and is a critical component in downstream signaling,[3] providing a high-affinity binding site for the SH2 domain of Src family kinases.[4,5] The interaction between Y397-activated FAK and Src leads to a cascade of tyrosine phosphorylation of multiple sites in FAK (FAK-576, -577, -925), as well as other signaling molecules such as $p130^{CAS}$ and paxillin, resulting in cytoskeletal changes and activation of other downstream signaling pathways.[6] Y397 is also a site of binding PI3 kinase, growth factor receptor binding Grb-7, Shc, and other proteins. Thus, the Y397 site is one of the main phosphorylation sites that activate FAK signaling in the cells.

Focal adhesion kinase is involved in multiple cellular functions such as cell proliferation, survival, motility, invasion, metastasis, and angiogenesis.[7] Different approaches to inhibit FAK with FAK antisense oligonucleotides,[8] dominant-negative C-terminal domain of FAK, FAK-CD or FRNK[9,10] or FAK siRNA,[11,12] caused decreased cellular viability, growth inhibition, or apoptosis. Recently, FAK was proposed to be a new potential therapeutic target in cancer.[13,14] Three novel kinase inhibitors of FAK, blocking FAK catalytic activity, were developed and reported recently, one by Novartis, **1a** (2-[5-chloro-2-[2-methoxy-4-(4-morpholinyl)phenylamino]pyrimidin-4-ylamino]-*N*-methylbenzamide, NVP-TAE226 (TAE226)),[15−17] and another two by Pfizer, **2a** (6-(4-(3-(methylsulfonyl)benzylamino)-5-(trifluoromethyl)pyrimidin-2-ylamino)-3,4-dihydroquinolin-2(1*H*)-one, $C_{22}H_{20}F_3N_5O_3S$ (PF-573,228 or PF-228))[18] and **3a** (*N*-methyl-*N*-(3-{[2-(2-oxo-2,3-dihydro-1*H*-indol-5-ylamino)-5-trifluoromethylpyrimidin-4-ylamino]methyl}pyridin-2-yl)methanesulfonamide (PF-562,271)).[19] The first inhibitor, **1a**,[16] inhibited glioma and ovarian tumor growth in vivo,[16,17] although it also inhibited IGFR kinase.[17] The efficacy of the **2a**[18] inhibitor on tumor growth in vivo has not been reported; it inhibited only motility and did not inhibit cell growth and survival in vitro.[18] **3a**[19] inhibitor effectively blocked kinase activity of FAK and decreased tumor growth.[19] All inhibitors effectively blocked Y397-FAK autophosphorylation.

Since the Y397 site is important for FAK survival function, we performed a computer modeling approach, described in ref 20, to specifically target the Y397-site of FAK and to find potential small-molecule compounds that inhibit FAK function and decrease cell viability and tumor growth.

To identify a novel FAK inhibitor, we employed computer modeling and functional approaches. We used DOCK 5.1 program and tested 140 000 small molecule compounds to target the Y397 site of FAK. We found that compound **14** targets the Y397 site directly and specifically decreases Y397 phosphorylation of FAK in vitro, inhibits cancer cell viability in vitro, causes detachment, decreases cell adhesion, and blocks tumor growth in vivo. Thus, targeting the Y397 site can be an effective therapy approach for developing future novel FAK inhibitors.

Materials and Methods

Cell Lines and Culture. BT474 breast carcinoma cells were maintained in RPMI1640 medium supplemented with 10% fetal bovine serum (FBS), 5 μg/mL insulin, and 1 μg/mL penicillin/streptomycin. The MCF-7 cell line was obtained from ATCC and maintained according to the manufacturer's protocol. Other cancer and normal cell lines were maintained according to ATCC protocol.

Structure-Based in Silico Molecular Docking of FAK Small-Molecule Inhibitors. We used a structure-based approach combining molecular docking with functional testing. The 140 000

* To whom correspondence should be addressed. Address: Department of Surgery, Health Science Center, University of Florida, P.O. Box 100286, 1600 SW Archer Road, Gainesville, FL 32610-0286. Phone: 352-265-0609. Fax: 352-338-9809. E-mail: cance@surgery.ufl.edu.

† Department of Surgery.

‡ UF Shands Cancer Center.

§ Department of Pathology and Laboratory Medicine.

|| Department of Biochemistry and Molecular Biology.

[a] Abbreviations: FAK, focal adhesion kinase; PARP, poly ADP-ribose polymerase; FAK-CD (FRNK), C-terminal domain of focal adhesion kinase.

10.1021/jm800483v CCC: $40.75 © 2008 American Chemical Society
Published on Web 11/07/2008

Table 1. Top Scoring Y397 Targeting Compounds

compd no.	compd label	NSC	formula	molecular weight
1	Y2	47228	$C_4H_{12}N_4$	116
2	Y3	53040	$C_9H_{12}N_6$	204
3	Y4	55937	$C_4H_{12}N_6$	144
4	Y5	66330	$C_2H_6N_4S$	118
5	Y6	81462	$C_9H_{18}N_4$	182
6	Y7	87061	$C_{15}H_{24}N_4$	26
7	Y8	100649	$C_6H_{18}N_4 \cdot 3ClH$	256
8	Y9	168639	$C_9H_{16}BrN_4 \cdot C_9H_{16}BrN_4 \cdot 2Br$	680
9	Y10	77977	$C_{16}H_{13}NO_5$	299
10	Y11	206142	$C_8H_{17}N_4O \cdot Br$	265
11	Y12	243780	$C_4H_{13}N_5 \cdot 2ClH$	204
12	Y13	337807	$C_4H_{12}N_4 \cdot 4BrH$	440
13	Y14	408480	$C_{16}H_{13}NO_5$	141
14	**Y15**	**667249**	**$C_6H_{10}N_4 \cdot 4ClH$**	**284**
15	Y17	10333	$C_7H_6FNO_2$	155
16	Y18	21220	$C_9H_{21}N_3O$	187
17	Y19	23434	$C_8H_{12}N_2O \cdot ClH$	189
18	Y20	26493	$C_4H_7N_5$	125
19	Y21	80640	$C_{13}H_{18}BrN_4 \cdot Br$	390
20	Y23	84628	$C_6H_{16}N_2O_4 \cdot 2BrH$	342
21	Y24	88220	$C_8H_{20}N_2O_2$	176
22	Y25	112847	$C_6H_{14}N_2O_2 \cdot 2ClH$	219
23	Y26	114704	$C_6H_4F_4N_2$	180
24	Y27	116289	$C_{14}H_{25}N_5O_2$	295
25	Y28	125186	$C_4H_8N_8$	168
26	Y29	145046	$C_4H_8N_4 \cdot ClH$	149
27	Y30	172826	$C_6H_{12}N_4O_2S$	204
28	Y31	175751	$C_5H_{10}N_6$	154
29	Y32	193871	$C_9H_{14}N_4O_2$	210
30	Y33	240745	$C_8H_{12}N_2O \cdot H_3O_4P$	250
31	Y35	281680	$C_4H_{12}N_4 \cdot 2ClH$	189
32	Y36	304712	$C_7H_{15}N_3OP \cdot I$	315
33	Y37	374666	$C_5H_{12}N_4O_2 \cdot ClH$	197
34	Y38	403347	$C_6H_{12}N_4 \cdot Cu$	204
35	Y39	664332	$C_9H_{16}BrN_4 \cdot Br$	340

small-molecule inhibitors following the Lipinski rules were docked into the N-terminal domain of FAK domain of the human FAK crystal structure in 100 different orientations using the DOCK 5.1 program, as described in ref 20. The crystal structure of FAK, N-terminal FERM domain[21] (PDB code 2AL6), was used for docking of FAK inhibitors. All water molecules were removed from the crystal structure, and SYBYL (Tripos, St. Louis, MO) was used to protonate and add charges to the residues. The spheres describing the target pocket of FAK were created using thenDOCK 5.1 suite program SPHGEN. Twenty-four spheres were ultimately selected to constrain small molecule orientations to within 5 Å of Y397 site. Docking calculations were performed on the University of Florida High Performance Computing supercomputing cluster using16 processors (http://hpc.ufl.edu).

Computational Docking. All docking calculations were performed with the University of California— San Francisco DOCK 5.1. program, using a clique-matching algorithm to orient small molecule structures with sets of spheres that describe the target Y397 site. Orientations were optimized using a simplex minimization algorithm, and 100 orientations were created for each small molecule in the target site that were independently scored using DOCK 5.1 grid-based scoring function. Briefly the three-dimensional coordinates of the 140 000 compounds of the National Cancer Institute, Developmental Therapeutics Program (NCI/DTP) database were obtained from NCI. The files for hydrogen atoms and partial charges were created using SYBDB program.

Small-Molecule Compounds. The top 35 compounds that were detected by the DOCK 5.1 program to best-fit into the Y397 site of FAK were ordered from the NCI/DTP database free of charge. Each compound was solubilized in water at 25 mM and stored at −20 and −80 °C. Compound **14** (shown in bold in Table 1) was ordered from Sigma for biochemical analyses in vitro and injection into mice and in vivo studies.

FAK Inhibitors. FAK kinase inhibitor **1a** was obtained from Novartis Inc.[16] FAK kinase inhibitor **2a** was obtained from Pfizer Inc.[18] Both **1a** and **2a** inhibitors were dissolved in DMSO at 25 mM. The structure and the therapeutic effect of the compound are described in refs 15−17. The **1a** and **2a** inhibitors were used as controls of FAK inhibition in the experiments.

Antibodies. Monoclonal anti-FAK (4.47) antibody to N-terminal FAK and monoclonal antipaxillin antibody were obtained from Upstate Biotechnology, Inc. Polyclonal anti-phospho-Tyr397-FAK, anti-phospho-Tyr118-paxillin, and anti-phospho-Tyr402-Pyk-2 were from Biosource, Inc. Total Pyk-2, paxillin, and PARP antibodies were from Cell Signaling, Inc. Monoclonal anti-β-actin antibodies were obtained from Sigma.

Cell Viability Assay. The cells were treated with compounds at different concentrations for 24 h. The 3-(4,5-dimethylthiazol-2-yl)-5-(3-carboxymethoxyphenyl)-2-(4-sulfophenyl)-2*H*-tetrazolium compound from the Promega Viability kit (Madison, IL) was added, and the cells were incubated at 37 °C for 1−2 h. The optical density on the 96-well plate was analyzed with a microplate reader at 490 nm to determine cell viability.

Propidium Iodide Staining. Treated compound cells were collected, and propidium iodide at 10 μg/mL in 1× PBS was added for 10 min. Hoechst 33342 (10 μg/mL) was added to the cells for detecting nuclei. Then cells were analyzed under a fluorescent microscope to detect dead propidium iodide-stained red cells.

Cell Adhesion Assay. The poly-L-lysine or collagen (5 μg/mL) coated 96-well plates were blocked with the blocking buffer (medium with 0.5% BSA) for 1 h at 37 °C. The cells were pretreated with the inhibitor for 3 h, collected, and plated for adhesion assay at 4×10^5 cells on a 96-well plate. Cells were incubated at 37 °C for 1 h, fixed in 3.7% formaldehyde, washed in 0.1% BSA in PBS, and stained with crystal violet (5 mg/mL in 2% ethanol) for 10 min. Then 2% SDS was added to the dried plated, and OD at 590 nm was measured for detecting cell adhesion.

Western Blotting. Cells or homogenized tumor samples were washed twice with cold 1× PBS and lysed on ice for 30 min in a buffer containing 50 mM Tris-HCl (pH 7.5), 150 mM NaCl, 1% Triton-X, 0.5% NaDOC, 0.1% SDS, 5 mM EDTA, 50 mM NaF, 1 mM $NaVO_3$, 10% glycerol, and protease inhibitors: 10 μg/mL leupeptin, 10 μg/mL PMSFm and 1 μg/mL aprotinin. The lysates were cleared by centrifugation at 10 000 rpm for 30 min at 4 °C. Protein concentrations were determined using a Bio-Rad kit. The boiled samples were loaded on Ready SDS−10% PAGE gels (Bio Rad, Inc.) and used for Western blot analysis with the protein-specific antibody. Immunoblots were developed with chemiluminescence Renaissance reagent (NEN Life Science Products, Inc.). For quantification, densitometry of protein bands was performed with NIH Scion Image software.

Immunoprecipitation. Immunoprecipitation was performed according to the standard protocol. In brief, the precleared lysates with equal amount of protein were incubated with 1 μg of primary antibody and 30 μL of A/G agarose beads overnight at 4 °C. The precipitates were washed with lysis buffer three times and resuspended in 2× Laemmli buffer. The boiled samples were used for Western blotting, as described above.

Detachment Assay. Cells were plated with and without inhibitors for 24 h, and detached and attached cells were counted in a hemocytometer. We calculated the percent of detachment by dividing the number of detached cells by the total number of cells. The percent of detached cells was calculated in three independent experiments.

Apoptosis Assay. Detached cells were collected and fixed in 3.7% formaldehyde in 1× PBS solution for the apoptosis assay. Detection of apoptosis was done with Hoechst 33342 staining. The percent of apoptotic cells was calculated as a ratio of apoptotic detached cells divided by the total number of cells in three independent experiments in several fields with the fluorescent microscope. For each experiment 300 cells per treatment were counted.

In Vitro Kinase Assay. For in vitro kinase assay and detecting FAK autophosphorylation activity, 0.1 μg of purified full length FAK protein was used in a kinase buffer (20 mM HEPES, pH 7.4, 5 mM $MgCl_2$, 5 mM $MnCl_2$) with 10 μCi of [γ-^{32}P]ATP. For

detecting FAK kinase activity, GST-paxillin^{N1C3} protein, the N-terminal paxillin domain containing the two binding sites for FAK, called GST-paxillin (a kind gift of Dr. M. Schaller, UNC, Chapel Hill, NC), was used for in vitro kinase assay. GST-paxillin (2.7 μg) was added as a substrate in the above kinase reaction. The kinase reaction with FAK alone or with FAK and paxillin was performed for 10 min at room temperature and stopped by addition of 2× Laemmli buffer. Isolated Pyk-2 protein was used in a kinase buffer (50 mM Tris, pH 7.5, 5 mM $MgCl_2$, 5 mM $MnCl_2$, 10 μM ATP) with 10 μCi [γ-^{32}P]ATP. The kinase reaction was performed as described above. Proteins were separated on a Ready SDS−10% PAGE gel. The gels were fixed in 7% acetic acid and 20% methanol and dried. The phosphorylated protein bands were visualized by autoradiography.

Kinase Profiler Screening. Kinase specificity screening was performed with KinaseProfiler Service (Millipore) available on http://www.millipore.com/drugdiscovery/dd3/KinaseProfiler. The screening was performed with 1 μM compound **14**, 10 μM ATP, and kinase substrates on nine recombinant kinases according to Millipore protocol (http://www.millipore.com/drugdiscovery/dd3/KinaseProfiler).

Tumor Growth in Nude Mice in Vivo. Female nude mice, 6 weeks old, were purchased from Harlan Laboratory. The mice were maintained in the animal facility, and all experiments were performed in compliance with NIH animal-use guidelines and IACUC protocol approved by the UF Animal Care Committee. BT474 cells were injected, 2×10^6 cells/injection subcutaneously. In preliminary experiments different doses of the compound were introduced into the mice, and 30 mg/kg was chosen as optimal, nontoxic dose. The day after injection, the compound was introduced by ip injection at 30 mg/kg dose daily 5 days/week for 3 weeks. Tumor diameters were measured with calipers, and tumor volume in mm^3 was calculated using the formula $(\text{width})^2 \times \text{length}/2$. At the end of experiment, tumor weight and volume was determined.

Immunohistochemistry and Immunostaining. FAK staining was performed with Y397 antibody on slides with paraffin-embedded tumor samples or on coverslips with fixed cells, as described previously.[22]

Statistical Analyses. Student's *t* test was performed to determine significance. The difference between data with $P < 0.05$ was considered significant.

Results

Targeting Y397 site of FAK by structure-based molecular docking approach and NCI database screening reveals Y397 compound that significantly decreased cell viability. The crystal structure of the N-terminal (FERM) domain of FAK has been recently identified[21] and was available in Protein Data Bank. Instead of high-throughput screening, we used a rapid structure-based approach combining molecular docking and functional testing. More than 140 000 compounds with known three-dimensional structure were docked into the structural pocket of FAK containing Y397 site. This approach combined the NCI/DTP (atomic coordinates and small molecules) database with improved molecular docking and scoring algorithms of the DOCK 5.1 program.[20] Each of 140 000 small-molecule compounds was docked in 100 different orientations using DOCK 5.1.0. As an example, one of such docked compounds in the Y397 site of FAK is shown in Figure 1A,B. Of more than 1 400 000 compounds, the 35 compounds that had the highest scores of binding energy of interaction with Y397 site of FAK (Table 1) were ordered from NCI and tested for the effect on cancer cell viability by MTT assay.

We tested six different cancer cell lines: BT474, T47D, MCF-7 breast cancer, HT29 colon cancer, C8161 melanoma, and A549 lung cancer cell lines with the 35 compounds, targeting the Y397 site of FAK. One of these compounds, compound **14** (labeled Y15 in bold, Table 1), maximally decreased cell viability in all cancer cell lines (Figure 1C,D). Compound **14** decreased viability in T47D breast cancer (Figure 1C) and C8161 melanoma cancer cells (Figure 1D) and is compared with the known FAK catalytic inhibitor **1a**[16] from Novartis, Inc. Some compounds such as compounds **19** and **27** (Table 1) decreased viability of some cancer cell lines (melanoma C8161 cell line, Figure 1D), but the effect was less in other cancer cell lines (Figure 1C) because of cancer and cell type specific differences. Importantly, compound **14** was effective on all tested cancer cell lines. The structure of compound **14**, docking to Y397 site, and the chemical name of this compound are shown in Figure 2A. The predicted model of compound **14** interaction with Y397 site of FAK is shown in Figure 2B with four hydrogen bonds (red dashed lines and one hydrophobic interaction (blue dashed line). Compound **14** with molecular weight of 284 and chemical formula shown in Table 1 was ordered from Sigma for the functional studies (below).

Compound 14 inhibits cancer cell viability in a dose-dependent manner. To determine whether **14** inhibits cell viability in a dose-dependent manner, MTT assay was performed with different doses: 0, 0.1, 1, 10, 30, 50, and 100 μM compound **14** (Figure 3A). The viability of BT474 cells started to decrease at 10 μM dose and was significantly blocked at 50−100 μM doses of **14** inhibitor. The inhibitor **14** was less effective in several normal cells: breast epithelial MCF10A cells and normal fibroblast cell lines compared with BT474 cell line (not shown). Thus, **14** blocks cancer cell viability in a dose-dependent manner.

Compound 14 specifically blocks Y397-FAK phosphorylation. To test the effect of **14** on Y397 phosphorylation, we treated BT474 breast cancer cells with **14** at 100 μM dose and performed Western blotting with Y397 FAK antibody (Figure 3B, left upper panels). Compound **14** specifically inhibited Y397 phosphorylation of FAK and also phosphorylation of FAK downstream substrate paxillin, Y118-paxillin (Figure 3B, upper panel). **14** did not inhibit phosphorylation of other proteins, such as VEGFR-3 and c-Src (not shown). In addition, we performed immunostaining of FAK with Y397-FAK antibody on BT474 cells, treated with **14** (Figure 3B, right upper panel). **14** significantly decreased Y397-FAK phosphorylation on attached cells. Thus, the effect of **14** was specific to FAK. To test the effect of **14** on total FAK autophosphorylation activity, we immunoprecipitated FAK and performed Western blotting with P-tyrosine antibody (Figure 3B, left lower panels). **14** inhibited total phosphorylation of FAK. Thus, **14**, which targets Y397 of FAK and decreases cell viability, specifically inhibits Y397 and total FAK phosphorylation.

Compound 14 blocks FAK autophosphorylation in a dose-dependent manner. Next we analyzed the effect of **14** on inhibiting FAK Y397 phosphorylation in a dose-dependent manner. We treated BT474 breast cancer cells with 0, 0.1, 1, 10, 50, and 100 μM **14** for 24 h and performed Western blotting with Y397 antibody (Figure 3C). The decreased Y397-FAK phosphorylation was observed at 10 μM dose, and **14** decreased Y397 phosphorylation in a dose-dependent manner with high and maximal inhibition detected at 50 and 100 μM doses, respectively, which is consistent with the effect on cell viability. At 100 μM dose **14** had the same FAK inhibition as **1a**[16] (Novartis) (Figure 3C). To detect the effect of **14** on autophosphorylation activity of FAK homologue Pyk-2, we performed Western blotting with Y402-Pyk2 antibody. Importantly, **14** did not inhibit Y402-Pyk2 levels compared to Y397-FAK level (Figure 3C). High doses of **14** (100 μM) decreased also the

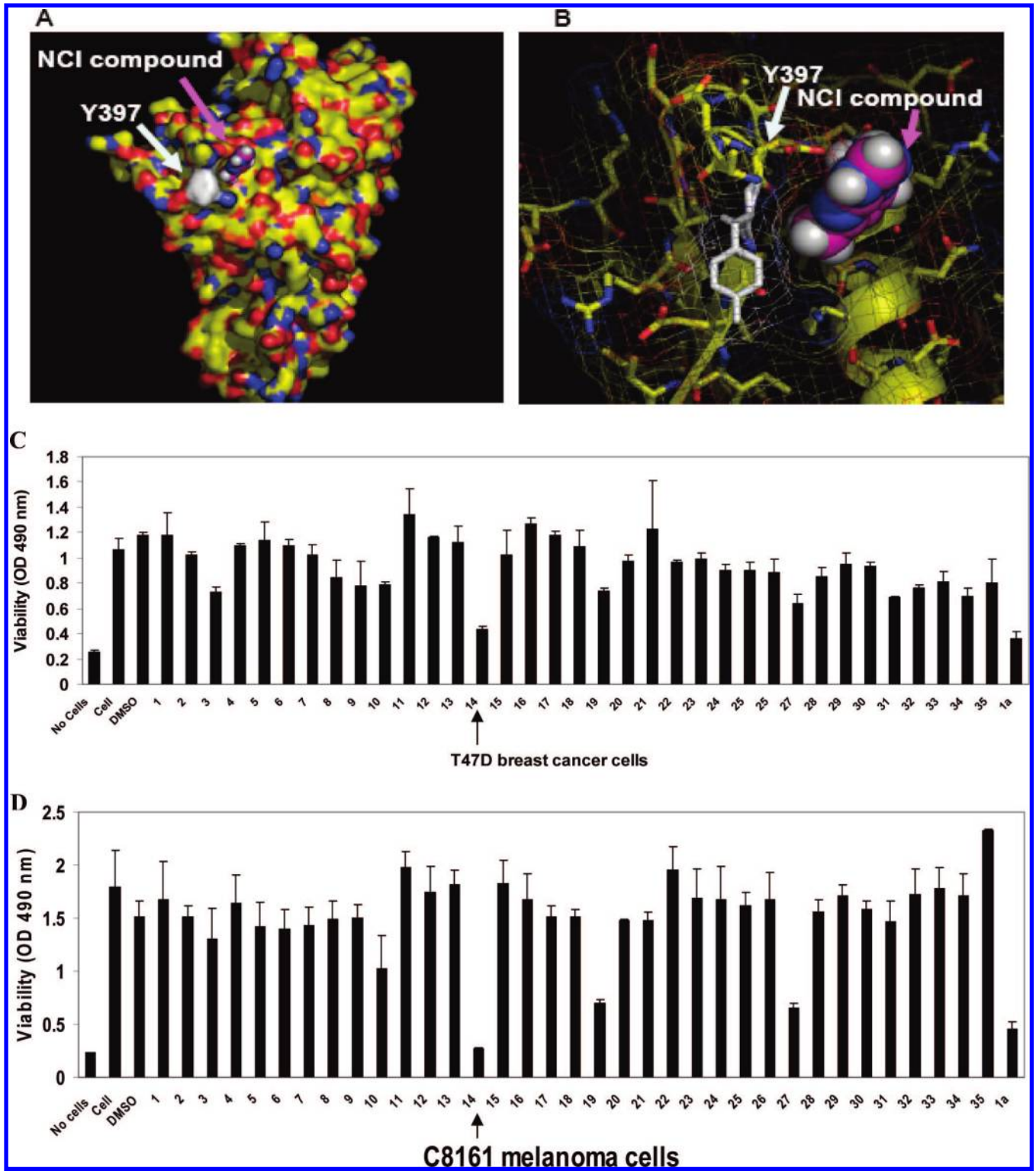

Figure 1. (A, B) Targeting of Y397 site of FAK by structure-based molecular docking approach: (A) crystal structure of FAK (FERM) domain, reported in ref 21, with one of the NCI compound targeting Y397 site of FAK (shown by arrows); (B) zoomed image of Y397 site and this example compound. (C, D) Effect of compounds targeting Y397 site on viability of breast cancer and melanoma cell lines. (C) The 35 compounds, **1**−**35** (Table 1), were added to the cells for 24 h at 100 μM dose, and MTT assay was performed, as described in Materials and Methods. The known FAK inhibitor, **1a**[16] (Novartis), was used as a control. Shown are results from T47D breast cancer cell line (C) and C8161 melanoma cell line (D). Bars show mean values ± standard deviations. Compound **14** decreased maximally cancer cell viability (shown by arrow).

level of total Pyk-2 and FAK, similar to **1a** inhibitor. Thus, **14** inhibits FAK autophosphorylation in a dose-dependent manner.

Compound 14 blocks FAK autophosphorylation in a time-dependent manner. Next we analyzed whether **14** inhibits FAK Y397 phosphorylation in time-dependent manner. We treated BT474 cells with 100 μM **14** for 0, 1, 4, 8, and 24 h. Then Western blotting was performed with Y397 antibody (Figure 3D). The result shows that treatment with **14** at 4 h did not significantly decrease Y397 phosphorylation, but 8 h was enough to completely block Y397-phosphorylation and to down-regulate FAK. The control inhibitors **1a**[16] at 100 μM also completely blocked Y397 phosphorylation. Similar to **14** inhibitor, **1a**[16] also

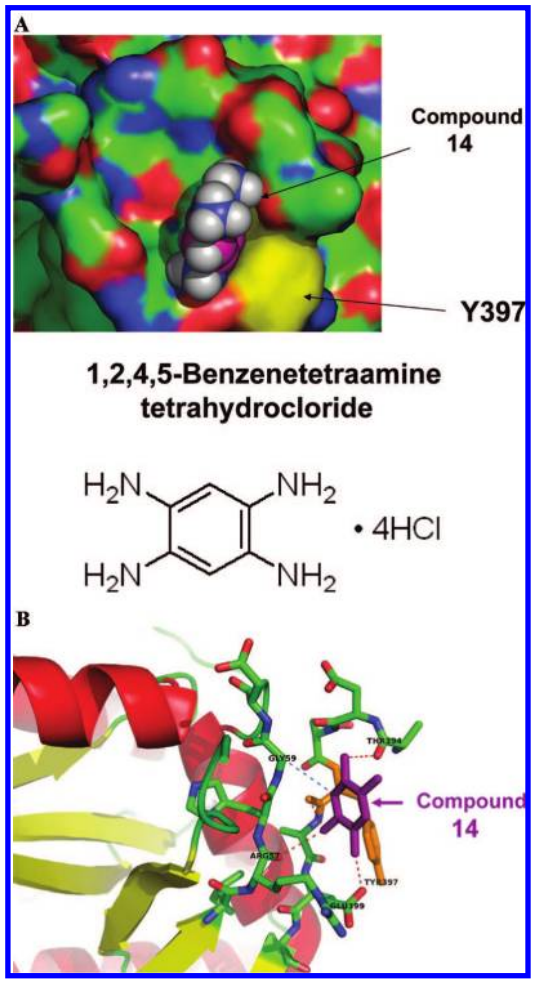

Figure 2. (A) Structure of **14**: (upper panel) compound **14** targets Y397 site of FAK; (lower panel) chemical structure and name of **14**. (B) Closeup view of compound **14** interaction in the Y397 site of FAK. The secondary structure of α helices and β sheets of the FAK-N-terminal domain are shown. **14** is shown in purple. The red dashed lines show hydrogen bonds, and blue dashed line shows hydrophobic interaction. Y397 residue is shown in orange.

down-regulated total FAK (Figure 3D). We performed densitometry analysis of **14**-treated cells and show that **14** decreased more Y397-FAK level than total FAK (Figure 3E). Thus, the data demonstrate that **14** inhibits FAK Y397 phosphorylation and down-regulates FAK in a time-dependent manner.

Compound 14 is a direct FAK autophosphorylation inhibitor. To test whether **14** is a direct inhibitor of FAK, we performed in vitro kinase assay with recombinant isolated with Baculovirus system purified FAK protein, described in ref 23. We performed in vitro kinase assay with 1−100 μM doses of **14**. We used **1a**[16] inhibitor as a positive control. **14** directly blocked autophosphorylation activity of FAK starting from 1 μM dose, as well as control **1a**[16] (Figure 4A, upper panel). In addition, we performed in vitro kinase assay with 1−100 μM doses of **14** and a recombinant baculoviral purified Pyk-2 protein, homologous to FAK, described in ref 23. **14** did not significantly block autophosphorylation activity of Pyk-2 compared to FAK activity (Figure 4A, lower panel). **14** did not significantly inhibit Pyk-2 at high 100 μM dose in contrast to **1a**[16] inhibitor. The amount of **14** required to inhibit >50% of the FAK autophosphorylation (IC_{50}) in this assay is about 1 μM.

To test whether inhibition of FAK autophosphorylation activity will affect FAK kinase activity, we used paxillin as a substrate and performed in vitro kinase assay, as described in Materials and Methods) (Figure 4B). FAK effectively phosphorylates paxillin in vitro (Figure 4B, lane 3). **14** inhibited FAK autophosphorylation and paxillin phosphorylation starting with 1 μM dose (Figure 4B). Thus, **14** blocked FAK autophosphorylation and kinase activity of FAK. In addition, **14** was screened by in vitro kinase assay with nine other recombinant commercially available kinases (c-RAF, c-Src, EGFR, VEGFR-3, IGF-1, Met, PDGFR-α, Pyk2 (homologue of FAK), PI3K (p110δ/p85α) (Upstate Biotechnology, Inc.), as described in Materials and Methods (Figure 4C). In this assay, **14** significantly decreased catalytic activity of the full length FAK, while it did not significantly affect kinase activities of the other kinases (Figure 4C). **14** did not decrease kinase activity of the FAK kinase domain (411−686 aa) with the deleted N-terminal domain, containing Y397 site, and did not affect kinase activity of the FAK homologue, Pyk2 protein (Figure 4C). Thus, **14** is a direct and specific inhibitor of FAK Y397-phosphorylation.

Compound 14 causes dose-dependent cell detachment in cancer cells. To test the effect of **14** inhibitor on breast cancer cells, we treated BT474 cells with **14** at 1 and 100 μM for 24 h. We performed analysis of detachment and apoptosis in **14**-treated BT474 cells and compared them with TAE-226-treated cells (Figure 5A). **14** caused dose-dependent detachment in BT474 cells (Figure 5A). At 10 μM dose, **14** caused only 8% detachment in BT474 cells, while at 50 μM dose, detachment was equal to 38%. At 100−200 μM doses, detachment reached 64%−66%. **14** caused less detachment than **1a**[16] inhibitor, which induced 30% detachment at 10 μM and >80% detachment at 50 μM dose. Thus, **14** effectively caused dose-dependent cellular detachment. In addition, we performed analysis of cell detachment in normal mammary epithelial MCF-10A cells (Figure 5B). **14** caused less detachment in MCF10A cells than in BT474 cells at high 100 μM dose (15% in MCF10A cells versus 64% in BT474 cells) (Figure 5B, upper panel). The morphology of MCF10A cells treated with **14** at 100 μM dose is shown in Figure 5B, lower panel. Thus, normal MCF10A breast cells are less detached than breast cancer BT474 cells (Figure 5B).

Compound 14 causes less apoptosis than 1a inhibitor. To test the effect of **14** on apoptosis, we performed Hoechst staining on untreated and **14**-treated cells. At high 50−100 μM dose, **14** did not cause significant apoptosis in BT474 cells, with apoptotic levels less than 5% (Figure 5C). In contrast, **1a** inhibitor (Novartis)[16] caused higher levels of apoptosis than **14**, which were equal to 35% at 10 μM and reached 69% at 20 μM dose (Figure 5C). Hoechst stained nuclei of **14** and **1a**[16] treated cells are shown in Figure 5D. No apoptotic nuclei were detected in treated cells with **14** at 100 μM dose in contrast to **1a**-treated cells at 20 μM doses (Figure 5D, upper panel). To confirm apoptosis data, we performed analysis of PARP cleavage in **14**-treated and **1a**-treated cells (Figure 5D, lower panel). **1a**-treated cells had cleaved PARP 89 kDa fragment starting at 1 μM dose, while cells treated with **14** did not have the cleaved PARP 89 kDa protein. At 10−20 μM doses, **14**-treated cells had significantly less cleaved 89 kDa PARP than **1a**-treated cells (Figure 5D, lower panel). At high 100 μM dose, both **14** and **1a** treated cells expressed less uncleaved 116 kDa PARP (Figure 5D, lower panel). However, **14**-treated cells did not express cleaved 89 kDa PARP protein in contrast to **1a**-treated apoptotic cells (Figure 5D, lower panel). **14**-treated cells expressed 55 kDa cleavage PARP fragments (not shown) that have been reported to be present in necrotic cells. To detect necrosis and confirm decreased viability data in **14**-treated BT474 cells at 100 μM dose, we stained the cells with propidium iodide, which detects

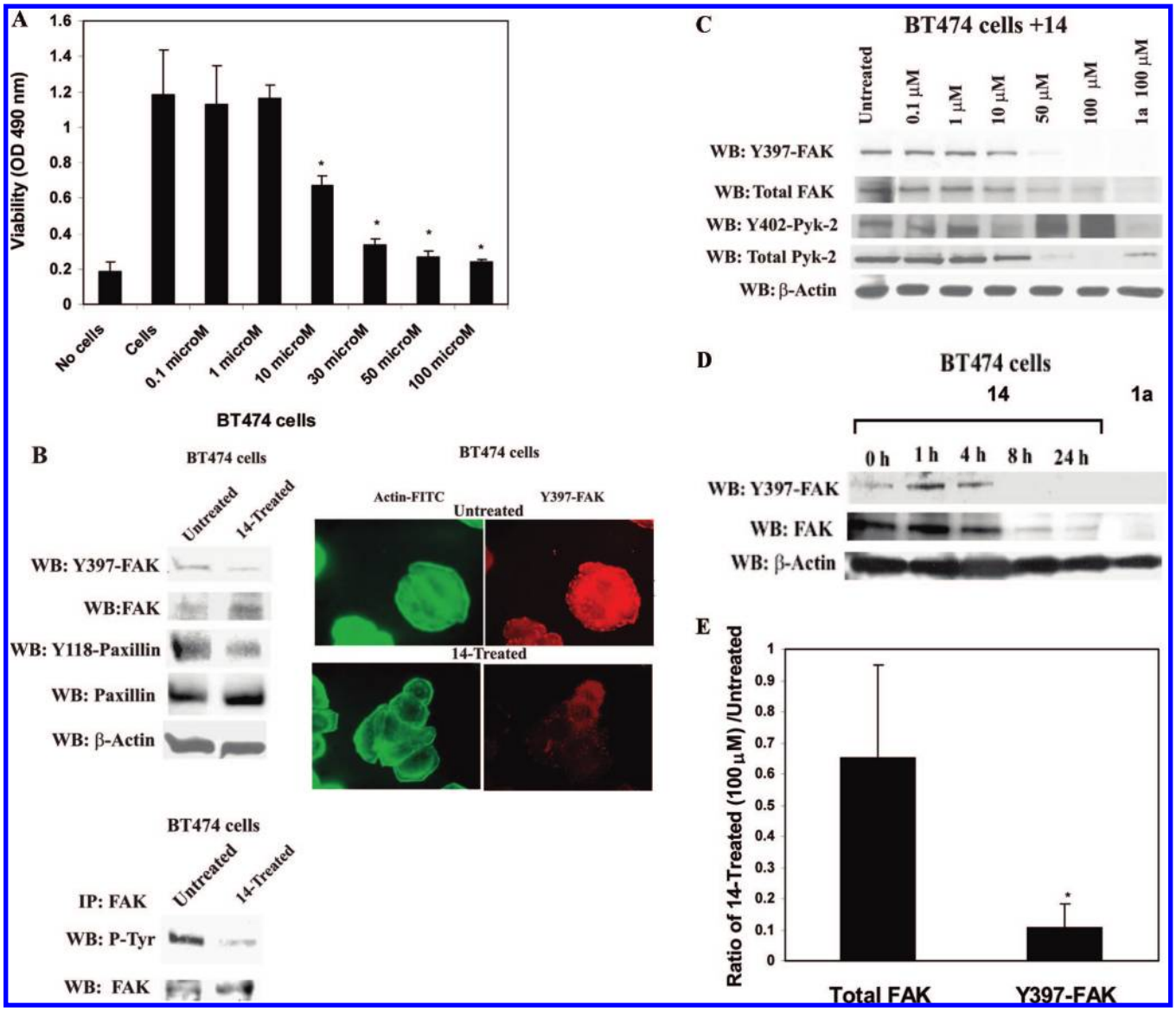

Figure 3. (A−C) Compound **14** inhibits cell viability and decreases Y397 FAK phosphorylation in a dose-dependent manner. (A) BT474 breast cancer cells were treated with different doses of **14** inhibitor for 24 h, and MTT assay was performed to test the effect on cell viability. Bars show the mean of triplicate determinations ± standard deviations. **14** inhibits cell viability in a dose-dependent manner: (∗) $P < 0.05$ viability of **14**-treated cells versus control untreated cells. (B, left upper panel) **14** specifically inhibits Y397 phosphorylation of FAK. BT474 cells were treated with **14** at 100 μM for 24 h, and Western blotting with Y397 and Y118 paxillin antibodies was performed to detect the level of phosphorylated FAK and paxillin, respectively. Western blotting with total FAK, paxillin, and β-actin was performed to detect expression of proteins in the cells. **14** effectively inhibited phosphorylation of Y397 and FAK substrate, Y118-paxillin. (B, right upper panel) Immunostaining with Y397-FAK antibody was performed on BT474 cells either untreated or treated with **14** at 100 μM for 24 h. Immunostaining was performed with primary Y397-FAK antibody and rhodamine-conjugated secondary antibody. FITC-Bodipy^{FL}-phallacidin was used for actin staining. **14** significantly decreased Y397-FAK in **14**-treated cells. (B, left lower panel) **14** blocked total phosphorylation of FAK. Immunoprecipitation was performed with FAK antibody, and Western blotting with phosphotyrosine antibody was performed. The blot was stripped and probed with FAK antibody. **14** blocked phosphorylation of FAK. (C) **14** decreases Y397 phosphorylation in a dose-dependent manner. Cells were treated with different doses of **14** inhibitor, and Western blotting was performed with Y-397 and then with FAK antibody. Western blotting with Y402-Pyk-2 antibody was performed to detect Y402-Pyk-2 phosphorylation. Western blotting with β-actin antibody was performed to control equal protein loading. (D) Compound **14** inhibits FAK autophosphorylation in a time-dependent manner. Cells were treated with 100 μM **14** inhibitor for 1, 1, 4, 8, and 24 h. Treatment with **1a** inhibitor at 100 μM for 24 h was used as a control. Western blotting with Y397 was performed to detect Y397-FAK level. Then the blot was stripped and Western blotting with FAK and β-actin was performed. Compound **14** inhibits Y397-FAK phosphorylation in a dose-dependent manner. (E) Quantification of inhibition of Y397-phosphorylation, caused by **14**. Densitometry analysis was performed of **14**-treated and untreated cells at 100 μM dose at three independent experiments using Scion Image, NIH software. Total FAK and Y397-FAK were expressed relative to β-actin, and then the ratio of total FAK and Y397-FAK levels was calculated in treated cells and expressed relative to untreated cells. Bars show mean ratio of **14**-treated/-untreated cells ± standard errors: (∗) $p < 0.05$ Y397-FAK compared to total FAK.

necrotic dead cells. We found dose-dependent increase of propidium iodide stained cells, reaching a maximum at 100 μM dose (Figure 5E). Thus, **14** induces nonapoptotic cell death by necrosis at 100 μM dose that decreased viability in the cells. Thus, **14** inhibitor causes less apoptosis than **1a** inhibitor at 10−20 μM dose and induces necrosis at high 100 μM dose.

Compound 14 inhibits cell adhesion in a dose-dependent manner. To test the effect of **14** on cell adhesion, we treated BT474 with different doses of **14** and with 100 μM **1a**[16] on collagen-coated plates and measured adhesion. **14** inhibited cell adhesion in a dose-dependent manner (Figure 5F). Starting with 50 μM, cell adhesion was significantly decreased, which is

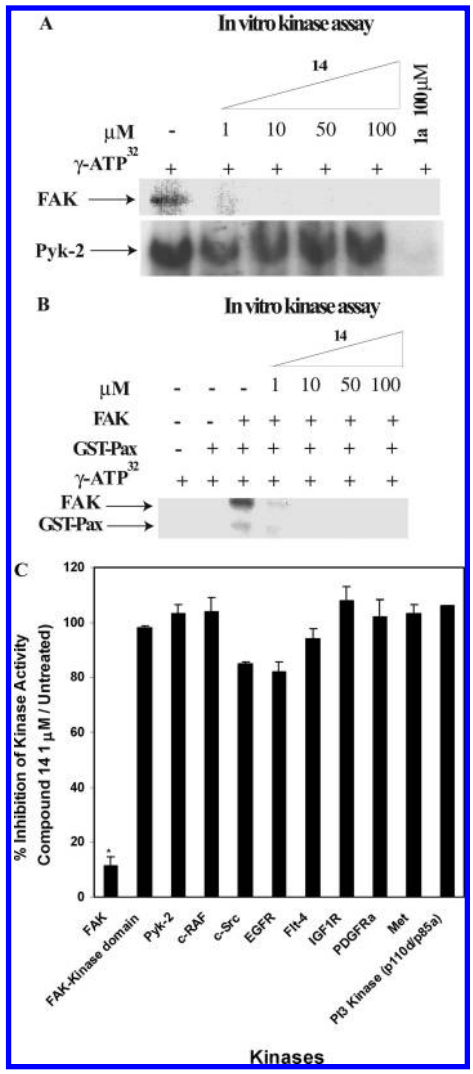

Figure 4. (A, B) Compound **14** directly blocks in vitro catalytic autophosphorylation and kinase activity of FAK. (A, upper panel) **14** blocks FAK catalytic autophosphorylation activity. In vitro kinase assay was performed with γ-ATP^{32}, 0.1 μg of purified recombinant FAK protein, and different doses of **14** inhibitor for 10 min at room temperature, as described in Materials and Methods. **14** directly blocks FAK autophosphorylation activity in a dose-dependent manner. (A, lower panel) **14** has no inhibiting effect on Pyk-2 catalytic autophosphorylation activity. In vitro kinase assay was performed with γ-ATP^{32}, 0.1 μg of purified recombinant Pyk-2 protein, and different doses of **14** inhibitor for 10 min at room temperature, as described in Materials and Methods. **14** did not significantly affect Pyk-2 autophosphorylation. The data are from three independent experiments. (B) Compound **14** blocks FAK kinase activity in vitro. GST-paxillin was added as a substrate in the kinase assay reaction. The reaction was performed with γ-ATP^{32}, 0.1 μg of purified recombinant FAK protein, and different doses of **14** inhibitor for 10 min at room temperature. **14** inhibits phosphorylation of paxillin in a dose-dependent manner. (C) Kinase profile of compound **14**. Compound **14** was screened against nine commercially available recombinant enzymes and catalytically active FAK kinase domain (411−686 aa) without the N-terminal domain, containing Y397 site by Kinase Profiller Service (Millipore/Upstate Biotechnology, Inc.). The assay was performed with 1 μM dose of **14** that inhibited activity of FAK (A, B), 10 μM ATP, and kinase substrates as described in Materials and Methods (http://www.millipore.com/drugdiscovery/dd3/KinaseProfiler). **14** effectively blocks full length FAK kinase activity (A, B), and it does not affect activities of homologous Pyk-2, FAK kinase domain, and other kinases. The bars show percentage of inhibition of the enzyme activity (**14**/untreated). The mean and standard errors of two independent experiments are shown.

consistent with Y397-decreased FAK phosphorylation at these doses. At 100 μM dose **14** significantly inhibited cell adhesion, as well as **1a** inhibitor (Figure 5F). Thus, **14** effectively blocks cell adhesion.

Compound 14 inhibits breast tumor growth in vivo and decreases Y397-FAK phosphorylation. To detect in vivo effect of **14**, we introduced BT474 cells subcutaneously into nude mice. Initially we determined that dose 30 mg/kg is the optimal nontoxic dose. We treated mice with 30 mg/kg dose of **14** for 5 days/week and compared tumor growth with untreated mice. No animal weight loss or death was observed in any tumor growth inhibition experiment for 23 days. **14** significantly blocked tumor growth in treated mice compared with untreated mice in vivo (Figure 6A). **14** significantly reduced tumor weight compared to untreated mice (Figure 6B, upper panel), and tumor volume was significantly less than in untreated samples (Figure 6B, lower panel). We isolated tumors from untreated mice and mice treated with **14** and probed for Y397 levels by Western blotting. Tumors from untreated mice had significantly higher levels of Y397 phosphorylation than tumors treated with **14**, while total FAK levels were the same (Figure 6C). A similar result was obtained by immunohistochemical staining of tumors with Y397 antibody (Figure 6D). Tumors from **14**-treated mice had less Y397-FAK phosphorylation than tumors from untreated mice. Thus, **14** significantly suppressed breast tumorigenesis, which is consistent with in vitro viability and biochemical data.

Discussion

FAK has been shown to be important for survival signaling, angiogenesis, motility, and metastasis and has been shown to be overexpressed in a number of tumors.[7] FAK was proposed recently to be a novel target for developing anticancer therapy drugs.[13] We developed a novel approach to target focal adhesion kinase by targeting its main autophosphorylation site by computer modeling and functional approaches. Thus, targeting Y397 of FAK with structure-based molecular docking and National Cancer Institute database screening approaches revealed 35 compounds out of 140 000 different compounds that best fit in this pocket. Among these compounds, compound **14** was the most effective in decreased cell viability in several cancer cell lines. Importantly, this compound decreased Y397 phosphorylation and total FAK phosphorylation. It directly decreased FAK autophosphorylation and inhibited FAK kinase activity on paxillin substrate in vitro. In BT474 cancer cells 50 μM **14** almost completely decreased FAK autophosphorylation. **14** decreased FAK phosphorylation in a dose- and time dependent manner. **14** increased cell detachment and decreased cell adhesion. In vitro kinase assay demonstrated that 1 μM dose of **14** was enough to significantly and specifically block FAK authophosphorylation and kinase activity. In cell culture a higher dose was required to inhibit Y397 phosphorylation, which can be explained by differences in sensitivity of Western blotting and in vitro radioactive kinase assay. Treatment with **14** induced cell detachment in BT474 cells. Importantly, that decreased phosphorylation of Y397-FAK occurred prior to significant detachment and cell death, as we detected decreased Y397 phosphorylation in **14**-treated attached cells. In addition in vivo, **14** significantly inhibited tumor growth at 30 mg/kg dose in BT474 breast cancer cells, subcutaneously injected in mice. Tumors from mice treated with **14** had decreased Y397 phosphorylation of FAK. Thus, **14** inhibitor, targeting Y397 site of FAK, can be affective inhibitor in anticancer therapy.

Thus, this report shows that the DOCK program shows proof-of principle for using silico-based strategies for identifying novel

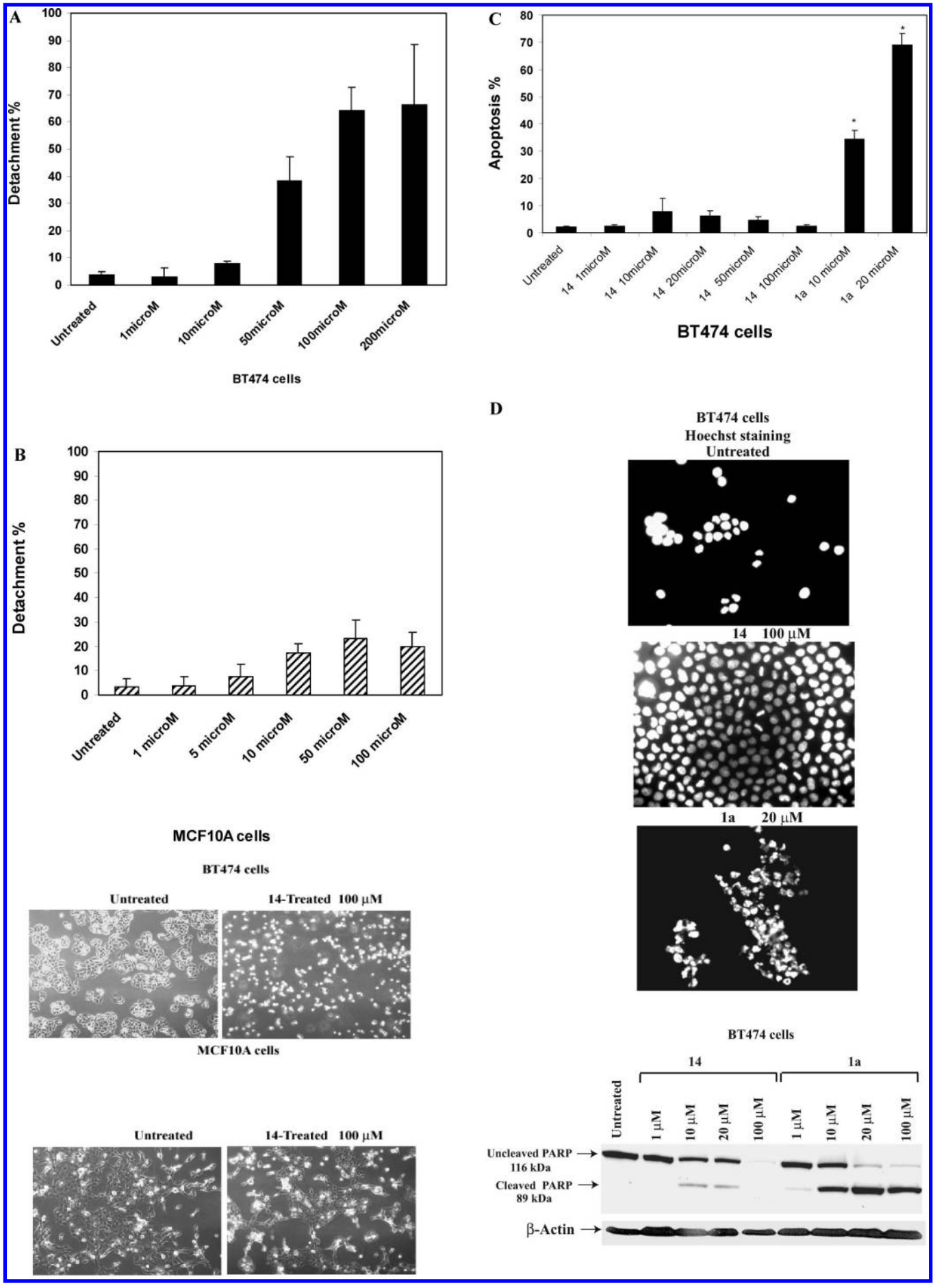
A
Detachment %
Untreated
1microM
10microM
50microM
100microM
200microM
BT474 cells
B
Detachment %
Untreated
1 microM
5 microM
10 microM
50 microM
100 microM
MCF10A cells
BT474 cells
Untreated
14-Treated 100 μM
MCF10A cells
Untreated
14-Treated 100 μM
C
Apoptosis %
Untreated
14 1microM
14 10microM
14 20microM
14 50microM
14 100microM
1a 10 microM
1a 20 microM
BT474 cells
D
BT474 cells
Hoechst staining
Untreated
14 100 μM
1a 20 μM
BT474 cells
14
1a
Untreated
1 μM
10 μM
20 μM
100 μM
1 μM
10 μM
20 μM
100 μM
Uncleaved PARP
116 kDa
Cleaved PARP
89 kDa
β-Actin

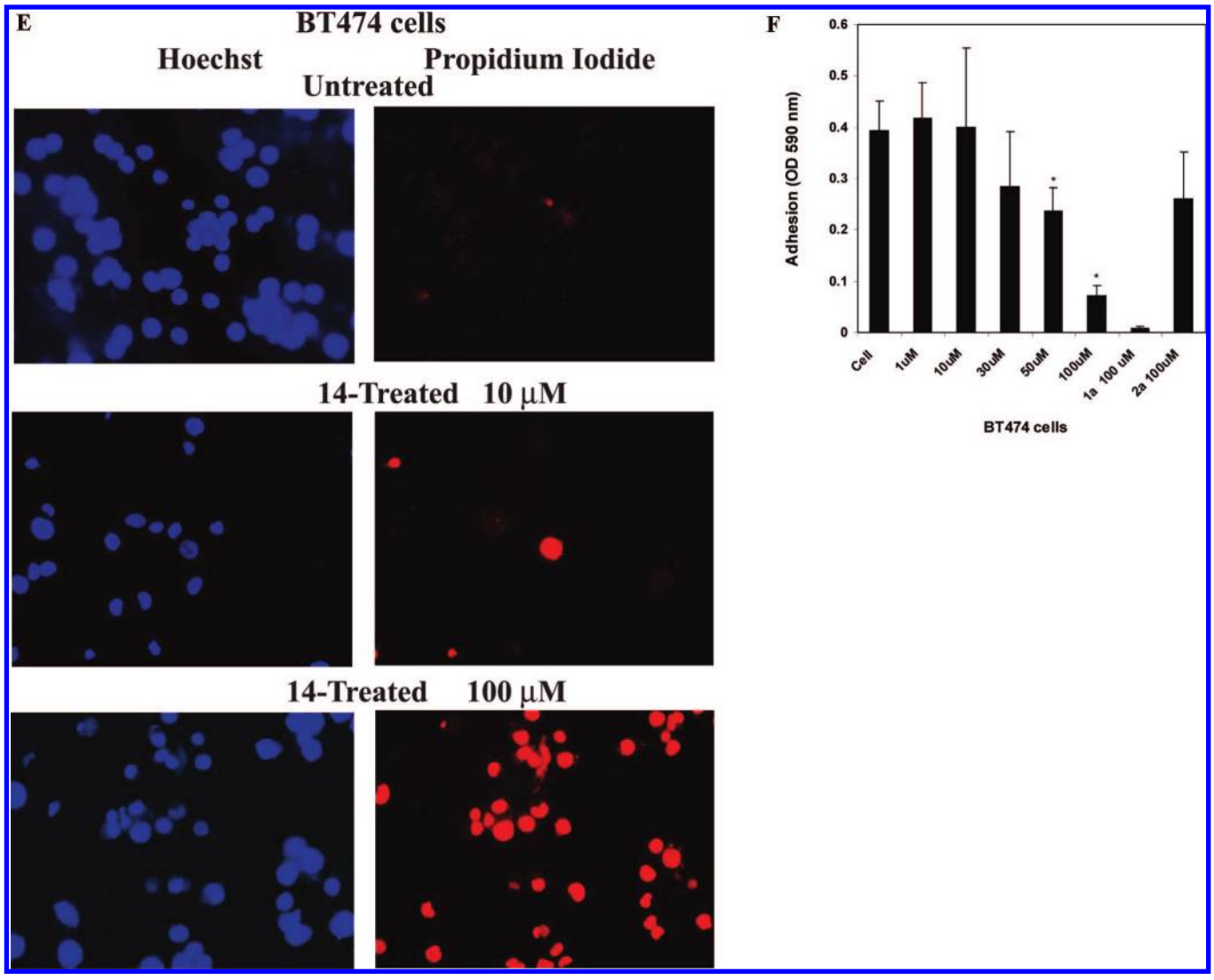

Figure 5. (A) Compound **14** causes dose-dependent cell detachment in BT474 cells. BT474 cells were treated with different doses of **14** inhibitor. The detachment was determined on a hemacytometer, as described in Materials and Methods. **14** significantly decreased cell detachment. Bars show mean values ± standard errors of three independent experiments: (∗) $P < 0.05$ versus untreated cells. (B) Detachment caused by **14** in normal breast MCF10A cells. (Upper panel) Normal breast MCF10A cells were treated with different doses of **14** inhibitor. The detachment was determined, as described in (A). Bars show means ± standard errors in three independent experiments. (Lower panel) A phase-contrast microscopy of MCF10A cells treated with **14** at 100 μM dose. Detachment is shown in BT474 and MCF10A cells treated with 100 μM **14**. No significant detachment was caused by **14** in MCF10A cells compared with BT474 cells. (C) Compound **14** does not cause significant apoptosis in BT474 cells. Hoechst staining was performed on BT474 cells at 24 h treatment with different doses of **14** and **1a**[16] inhibitors, as described in Materials and Methods. No significant apoptosis was detected with **14** compared to **1a** inhibitor. Bars represent means ± standard deviations in four independent experiments: (∗) $P < 0.05$ versus untreated cells. (D, upper panel) Hoechst staining of **14**-treated BT474 cells. BT474 cells treated as above were analyzed by Hoechst staining. Apoptotic nuclei stained with Hoechst are shown. No apoptotic nuclei were observed with **14** inhibitor at 100 μM dose compared to **1a**[16] inhibitor at 20 μM dose. (Lower panel) PARP cleavage in **14**-treated and **1a**-treated cells. Western blotting on BT474 cells, treated with **14** or **1a** inhibitors at different doses, was performed with PARP antibody. **1a** caused significantly higher levels of cleaved PARP (89 kDa) compared with **14**-treated cells. No cleaved 89 kDa PARP was detected at 100 μM dose in **14**-treated cells compared with **1a**-treated cells. (E) Propidium iodide staining of **14**-treated cells. BT474 cells treated with **14** at 10 and 100 μM as above were collected and stained for 10 min with 10 μg/mL propidium iodide, detecting dead necrotic cells, and with Hoechst (10 μg/mL), detecting nuclei. Cells were analyzed under a Zeiss fluorescent microscope. Propidium iodide staining was increased in a dose-dependent manner and reached a maximum at 100 μM dose. (F) Compound **14** blocks cell adhesion in a dose-dependent manner. BT474 cells were treated with **14** at different concentrations, and cell adhesion was measured as described in Materials and Methods. **1a**[16] and **2a**[18] inhibitors at 100 μM were used as a control. **14** significantly blocked cell adhesion in a dose dependent manner. Bars show mean values ± standard errors of four independent experiments: (∗) $P < 0.05$, cell adhesion in **14**-treated cells less than in untreated control cells.

inhibitors of FAK. This method was successfully used before for Jak2 kinase,[20] but for the FAK kinase and for targeting the main phosphorylation site of FAK it was never reported. We showed that using the DOCK 5.1 program in conjunction with functional testing, we can successfully identify novel small molecule inhibitors of FAK by database screening. It is possible to use this approach for testing other sites and pockets of FAK in future. Thus, screening compounds that target other phosphorylation can also provide novel inhibitors that can be potentially used in therapy.

The molecular structure of **14** is known, and it contains a single aromatic ring. Thus, this single aromatic ring compound can serve as a potential lead compound for future chemically synthesized derivatives and novel FAK inhibitors.

The most important finding is that **14** blocked tumorigenesis in mice in vivo, showing potential in therapy for these

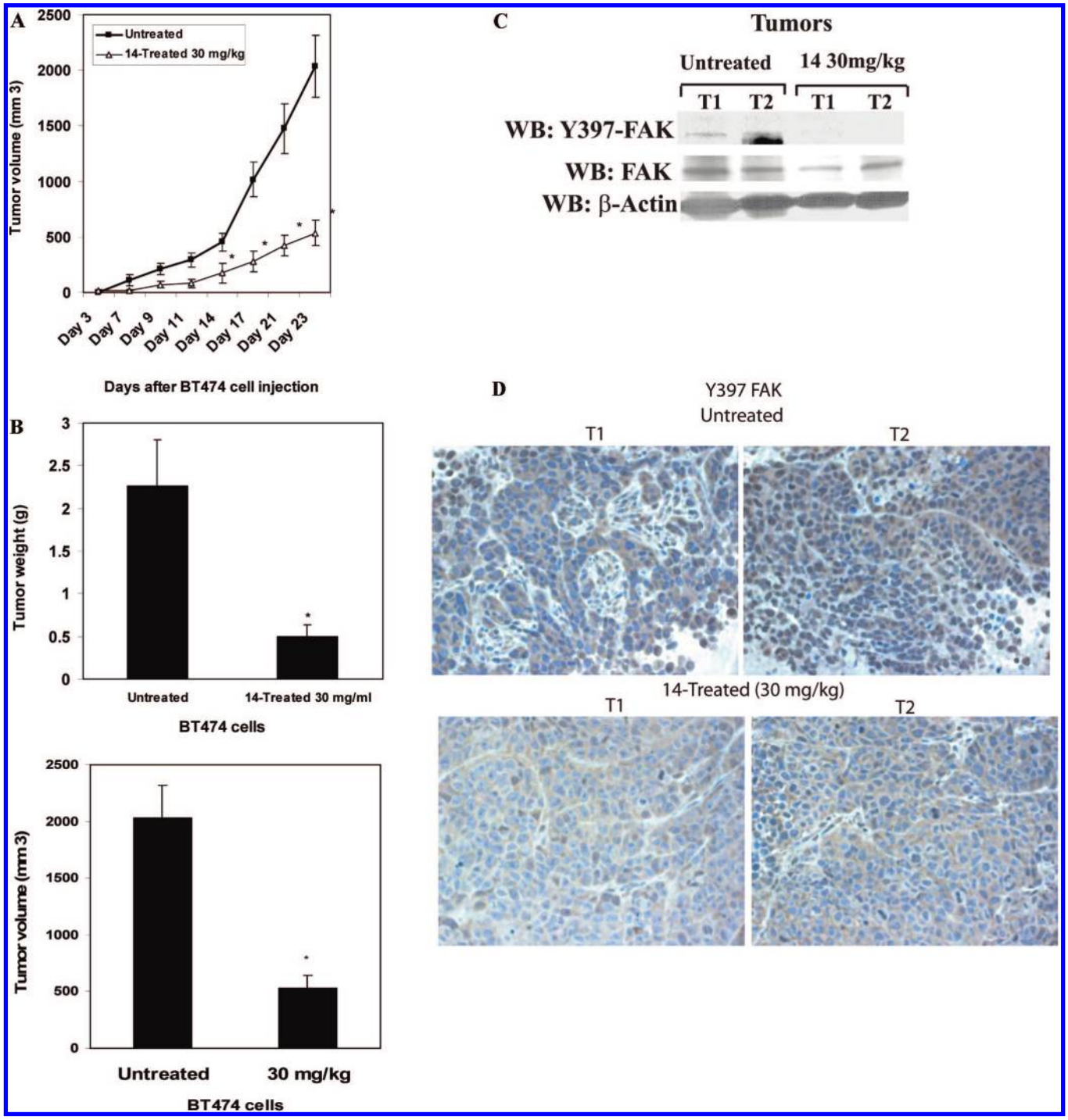

Figure 6. (A, B) Compound **14** significantly blocks tumor growth in vivo. (A) BT474 breast cancer cells were subcutaneously injected into five mice. The day after injection, **14** at 30 mg/kg was added daily 5 days per week. Five untreated mice were used as a control group. Tumor volume was measured with calipers. **14** significantly blocked tumor growth in vivo. Bars represent mean values ± standard deviations ($n = 5$): $P < 0.05$, Student's t test. (B) Compound **14** significantly blocks tumor weight and volume. At day 23 after breast cancer cell injection, tumors were extracted and weight and volume were determined in grams (upper panel) and in mm^3 (lower panel), respectively. **14** significantly blocked tumor weight (upper panel) and volume (lower panel). Bars represent mean values ± standard deviations: (∗) $p < 0.05$, Student's t test. (C, D) Compound **14** decreases Y397-FAK phosphorylation in tumors. (C) We isolated tumors from untreated mice and from mice treated with **14**. Cell lysates were prepared, and Western blotting was performed with Y397 antibody. FAK and β-actin antibodies were used for detecting total FAK and β-actin levels. (D) Immunohistochemical staining analysis was performed on untreated and **14**-treated tumors with Y397 antibody. Two representative tumors from untreated and **14** treated mice groups are shown (marked as T1 and T2 tumors in each group) (C, D). **14** decreased Y397FAK phosphorylation in tumors treated with **14** (30 mg/kg) compared with untreated mice.

inhibitors. Two other novel FAK inhibitors were reported, **2a**[18] by Pfizer and **1a**[16] by Novartis. Both inhibitors have their own limitations; the first inhibitor **2a** has no effect on cell viability, and no report on tumorigenesis is known. The second one, **1a** has an inhibiting effect on IGFR-1, MAPK, and AKT.[17] **1a** caused induced apoptosis in vitro.[15] In contrast, **14** did not cause significant apoptosis, similar to Pfizer inhibitor **2a**,[18] but caused detachment and loss of adhesion. The authors suggest that scaffolding function of FAK can be important in regulating apoptosis.[17] We detected

increased cell death by trypan blue (not shown) and propidium iodide staining in **14**-treated cells; thus, decreased viability caused by **14** can be explained by nonapoptotic mechanism such as necrosis, which will be studied in future reports. Since FAK and TNF receptor pathways are linked in cells,[7] the TNF-induced nonapoptotic cell death mechanism may be important in **14**-treated cells. Thus, **14** can have a therapeutic effect in apoptosis-resistant tumor cells. The difference between **14** and **1a** in causing apoptosis at 10−20 μM doses can be explained by higher specificity of **14** to FAK. For example, **14** did not inhibit kinase activity of IGFR, while **1a** has been shown to effectively inhibit IGFR-1 activity.[16] **14** also did not affect phosphorylation of PYK-2 homologue, which can be explained by only 43% amino acid identity between N-terminal domains of FAK and Pyk-2 proteins.[21] In addition, amino acids involved in interaction with **14** are not conserved between FAK and Pyk-2. We performed computer modeling and docking of **14** into the predicted PYK2 domain and found that **14** was not docked into the Pyk-2 structure, as well as into FAK. **14** is more specific than **1a**[16] inhibitor, as **1a** at 100 μM dose decreased Y402-Pyk-2 autophosphorylation, while **14** did not affect its activity. Increased selectivity of **14** to FAK but not to homologous Pyk-2 can be useful in the therapy of FAK-overexpressing tumors. **14** inhibitor blocked cell adhesion in a dose-dependent manner. The fact that **14** inhibited less cell adhesion and caused less detachment than **1a** inhibitor can be explained by less specificity of **1a** to FAK, as it cross-reacts with other kinases. Normal breast MCF10A cells were more resistant to **14** than cancer cells, similar to **1a**-caused detachment in MCF10A.[15] This can explain that tumors that overexpressed FAK were sensitive to **14** inhibitor in vivo. **14** specifically blocked Y397 phosphorylation of FAK, inhibited FAK kinase activity, and did not inhibit kinase activity of other enzymes. **14**, which targets Y397 site, blocked FAK autophosphorylation and phosphorylation of its substrate paxillin, which is consistent with data on critical role of Y397 site in phosphorylation of paxillin in vitro. **14** significantly blocked Y397 inside cancer cells at <50 μM, and 1 μM dose is enough to significantly block FAK autophosphorylation in a tube by in vitro kinase assay. Importantly, both assays demonstrated FAK as a specific target of **14**. The **14** and **1a**[16] inhibitors caused cell death by different mechanisms. **1a** caused more apoptosis than **14** becasue of differences in specificities. **14** blocked tumorigenesis at doses lower than **1a**.[16] In glioma tumors, **1a** was used at 50−75 mg/kg.[17] In the ovarian tumor model, **1a** alone at 30 mg/kg was not so effective and required additional docetaxel treatment to reduce tumor growth.[16] In the breast cancer model, **14** alone effectively inhibited >74% of tumor growth at 30 mg/kg dose. The third inhibitor of FAK **3a** from Pfizer[19] was effective in human xenograft models at doses 25−50 mg/kg that was accompanied by decreased FAK phosphorylation.[19] Thus, developing novel and more specific inhibitors of FAK that will block tumorigenesis is important to the field.

Thus, this report led to the identification of compound **14**, a small-molecule FAK inhibitor that directly targeted the Y397 autophosphorylation site of FAK and decreased its phosphorylation, inhibited cell viability and adhesion in vitro, and blocked tumorigenesis in vivo. Thus, this compound and its derivatives may be important for future therapies.

Acknowledgment. We thank Dr. Ann Dontao Fu and members from Molecular Pathology Core, Department of Pathology, UF, for technical help in immunohistochemical analysis of tumors. We acknowledge Dr. Shinji Hatakeyama (Novartis, Inc.) for providing the chemical name of **1a** inhibitor. We acknowledge the University of Florida High-Performance Computing Center for providing computational resourses and support. The work was supported by Susan G. Komen for the Cure Grant BCTR0707148 (V.M.G.) and NIH Grant CA65910 (W.G.C.).

References

(1) Schaller, M. D. The focal adhesion kinase. *J. Endocrinol.* **1996**, *150* (1), 1–7.
(2) Hildebrand, J. D.; Schaller, M. D.; Parsons, J. T. Identification of sequences required for the efficient localization of the focal adhesion kinase, pp125FAK, to cellular focal adhesions. *J. Cell Biol.* **1993**, *123* (4), 993–1005.
(3) Xing, Z.; Chen, H. C.; Nowlen, J. K.; Taylor, S. J.; Shalloway, D.; Guan, J. L. Direct interaction of v-Src with the focal adhesion kinase mediated by the Src SH2 domain. *Mol. Biol. Cell* **1994**, *5* (4), 413–421.
(4) Cobb, B. S.; Schaller, M. D.; Leu, T. H.; Parsons, J. T. Stable association of pp60src and pp59fyn with the focal adhesion-associated protein tyrosine kinase, pp125FAK. *Mol. Cell. Biol.* **1994**, *14* (1), 147–155.
(5) Schaller, M. D.; Hildebrand, J. D.; Shannon, J. D.; Fox, J. W.; Vines, R. R.; Parsons, J. T. Autophosphorylation of the focal adhesion kinase, pp125FAK, directs SH2-dependent binding of pp60src. *Mol. Cell. Biol.* **1994**, *14* (3), 1680–1688.
(6) Hanks, S. K.; Polte, T. R. Signaling through focal adhesion kinase. *BioEssays* **1997**, *19* (2), 137–145.
(7) Golubovskaya, V. M.; Cance, W. G. Focal adhesion kinase and p53 signaling in cancer cells. *Int. Rev. Cytol.* **2007**, *263*, 103–153.
(8) Smith, C. S.; Golubovskaya, V. M.; Peck, E.; Xu, L. H.; Monia, B. P.; Yang, X.; Cance, W. G. Effect of focal adhesion kinase (FAK) downregulation with FAK antisense oligonucleotides and 5-fluorouracil on the viability of melanoma cell lines. *Melanoma Res.* **2005**, *15* (5), 357–362.
(9) Xu, L.-h.; Yang, X.-h.; Bradham, C. A.; Brenner, D. A.; Baldwin, A. S.; Craven, R. J.; Cance, W. G. The focal adhesion kinase suppresses transformation-associated, anchorage-independent apoptosis in human breast cancer cells. *J. Biol. Chem.* **2000**, *275*, 30597–30604.
(10) Golubovskaya, V.; Beviglia, L.; Xu, L. H.; Earp, H. S., 3rd.; Craven, R.; Cance, W. Dual inhibition of focal adhesion kinase and epidermal growth factor receptor pathways cooperatively induces death receptor-mediated apoptosis in human breast cancer cells. *J. Biol. Chem.* **2002**, *277* (41), 38978–38987.
(11) Halder, J.; Landen, C. N., Jr.; Lutgendorf, S. K.; Li, Y.; Jennings, N. B.; Fan, D.; Nelkin, G. M.; Schmandt, R.; Schaller, M. D.; Sood, A. K. Focal adhesion kinase silencing augments docetaxel-mediated apoptosis in ovarian cancer cells. *Clin. Cancer Res.* **2005**, *11* (24, Part 1), 8829–8836.
(12) Beierle, E. A.; Trujillo, A.; Nagaram, A.; Kurenova, E. V.; Finch, R.; Ma, X.; Vella, J.; Cance, W. G.; Golubovskaya, V. M. N-MYC regulates focal adhesion kinase expression in human neuroblastoma. *J. Biol. Chem.* **2007**, *282* (17), 12503–12516.
(13) McLean, G. W.; Carragher, N. O.; Avizienyte, E.; Evans, J.; Brunton, V. G.; Frame, M. C. The role of focal-adhesion kinase in cancer—a new therapeutic opportunity. *Nat. Rev. Cancer* **2005**, *5* (7), 505–515.
(14) van Nimwegen, M. J.; van de Water, B. Focal adhesion kinase: a potential target in cancer therapy. *Biochem. Pharmacol.* **2007**, *73*, 597–609.
(15) Golubovskaya, V. M.; Virnig, C.; Cance, W. G. TAE226-induced apoptosis in breast cancer cells with overexpressed Src or EGFR. *Mol. Carcinog.* **2008**, *47*, 222–234.
(16) Halder, J.; Lin, Y. G.; Merritt, W. M.; Spannuth, W. A.; Nick, A. M.; Honda, T.; Kamat, A. A.; Han, L. Y.; Kim, T. J.; Lu, C.; Tari, A. M.; Bornmann, W.; Fernandez, A.; Lopez-Berestein, G.; Sood, A. K. Therapeutic efficacy of a novel focal adhesion kinase inhibitor TAE226 in ovarian carcinoma. *Cancer Res.* **2007**, *67* (22), 10976–10983.
(17) Liu, T. J.; LaFortune, T.; Honda, T.; Ohmori, O.; Hatakeyama, S.; Meyer, T.; Jackson, D.; de Groot, J.; Yung, W. K. Inhibition of both focal adhesion kinase and insulin-like growth factor-I receptor kinase suppresses glioma proliferation in vitro and in vivo. *Mol. Cancer Ther.* **2007**, *6* (4), 1357–1367.
(18) Slack-Davis, J. K.; Martin, K. H.; Tilghman, R. W.; Iwanicki, M.; Ung, E. J.; Autry, C.; Luzzio, M. J.; Cooper, B.; Kath, J. C.; Roberts, W. G.; Parsons, J. T. Cellular characterization of a novel focal adhesion kinase inhibitor. *J. Biol. Chem.* **2007**, *282* (20), 14845–14852.
(19) Roberts, W. G.; Ung, E.; Whalen, P.; Cooper, B.; Hulford, C.; Autry, C.; Richter, D.; Emerson, E.; Lin, J.; Kath, J.; Coleman, K.; Yao, L.; Martinez-

Alsina, L.; Lorenzen, M.; Berliner, M.; Luzzio, M.; Patel, N.; Schmitt, E.; LaGreca, S.; Jani, J.; Wessel, M.; Marr, E.; Griffor, M.; Vajdos, F. Antitumor activity and pharmacology of a selective focal adhesion kinase inhibitor, PF-562,271. *Cancer Res.* **2008**, *68* (6), 1935–1944.

(20) Sandberg, E. M.; Ma, X.; He, K.; Frank, S. J.; Ostrov, D. A.; Sayeski, P. P. Identification of 1,2,3,4,5,6-hexabromocyclohexane as a small molecule inhibitor of jak2 tyrosine kinase autophosphorylation [correction of autophophorylation]. *J. Med. Chem.* **2005**, *48* (7), 2526–2533.

(21) Ceccarelli, D. F.; Song, H. K.; Poy, F.; Schaller, M. D.; Eck, M. J. Crystal structure of the FERM domain of focal adhesion kinase. *J. Biol. Chem.* **2006**, *281* (1), 252–259.

(22) Golubovskaya, V. M.; Finch, R.; Kweh, F.; Massoll, N. A.; Campbell-Thompson, M.; Wallace, M. R.; Cance, W. G. p53 regulates FAK expression in human tumor cells. *Mol. Carcinog.* **2008**, *47*, 373–382.

(23) Golubovskaya, V. M.; Finch, R.; Cance, W. G. Direct interaction of the N-terminal domain of focal adhesion kinase with the N-terminal transactivation domain of p53. *J. Biol. Chem.* **2005**, *280* (26), 25008–25021.

JM800483V